

Retrograde motion in the carotid artery wall, the impact of left ventricle movement of the heart

Roger Persson F07
ner.persson@gmail.com

Electrical Measurements, Faculty of Engineering, LTH,
Lund University, Lund Sweden.

Tutor:
Magnus Cinthio
Associate Professor

Electrical Measurements, Faculty of Engineering, LTH,
Lund University, Lund Sweden.



LUND UNIVERSITY

Abstract

Cardiovascular diseases, such as atherosclerosis, is a major cause of mortality in, primarily, the western world. To be able to recognize early symptoms of this type of diseases it has proven to be important to investigate the mechanical properties of blood vessels. A few years back from now it became evident that the common carotid artery has a distinct bidirectional movement pattern in the longitudinal direction during each cardiac cycle. The mechanisms of this behavior has however since then been undetermined.

In this study three independent indicators of the cardiac wall movements' involvement is presented.

By ultrasound examinations of both the right and left side common carotids and simultaneous examinations of left ventricle movement of the heart of 14 humans it has become evident that:

The longitudinal movement in the carotid arterial wall, in both directions, occurs in parts of the vessel close to the heart before it is transmitted to more peripheral parts of the vessel.

In every instance, the movement of the heart precedes the movement in the carotids.

The motion forward on the right side carotid occurs before the motion forward on the left side.

All these pieces of evidence suggests that the heart's movement is the mother of, or at least significantly involved in, the longitudinal motion in the carotid arterial walls.

Contents

1	Introduction	2
1.1	Ultrasound	4
1.1.1	Wave propagation	4
1.1.2	Reflection	5
1.1.3	Attenuation	6
1.1.4	Transducer	6
1.1.5	Resolution	7
1.1.6	Modes	7
1.2	Echo tracking	8
2	Methods	9
2.1	Analysis	10
2.1.1	Heart movement	10
2.1.2	Carotid artery wall movement	11
2.1.3	Order of occurrence	14
3	Results	15
3.1	Movement	15
3.2	Order of occurrence	17
3.3	Side to side comparison	18
4	Discussion	19

1 Introduction

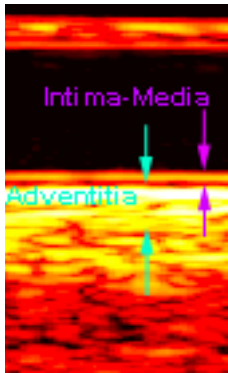


Figure 1: *The layers in the arterial wall.*

Cardiovascular diseases has for a long time been, and remains to be, the major cause of morbidity and mortality in the western world. To increase the knowledge about the underlying factors and symptoms of the disease it is, among other fields, important to investigate the mechanical properties of arteries¹. The mechanical properties, such as increased stiffness, of the arteries has proven² to give an early signal of manifestation of disease. The axial movements in arterial walls, i.e. the diameter change, has been extensively investigated and is nowadays a fundamental tool for estimation of arterial wall elasticity. The longitudinal movement of the arterial wall has although gained little attention. The motion has been regarded as of negligible magnitude in comparison with axial movement. The movement, nevertheless, exists and is actually of comparable magnitude of the axial deformation which has been reviewed and shown in previous articles³. The reason to the previous ignorance of this fact is most likely that

the movement has not been noticeable until recent improvements of the common ultrasound equipment used in hospitals. With modern high resolution ultrasound machines the motion is however quite noticeable.

The longitudinal movement in the arterial wall is usually measured in the “*intima-media complex*” of the vessel wall. The “*intima*” is the innermost layer of cells in the vessel and is in direct contact with the blood. Surrounding the intima is the “*media*”-layer which consists of smooth muscles and elastic tissue. The intima layer is generally not distinguishable from the media in ultrasound examinations; therefore, are the two layers commonly denominated the intima-media complex (IM). Surrounding the IM is the adventitia layer which is composed of connective tissue. Figure 1 shows an ultrasound image of the common carotid artery where the two layers are visible. The thickness of the adventitia can be hard to determine, so the lower arrow could be misleading.

The longitudinal movement of the IM in the common carotid artery has a specific pattern which is individually independent. The motion during the cardiac cycle has in a previous study³ of 10 healthy humans been determined to be of the kind:

An antegrade, i.e. in direction of blood flow, movement during early systole [0.39 mm (SD 0.26)] followed by a retrograde, i.e in direction opposite to blood flow, motion [-0.52 mm (SD 0.27)] in late systole and eventually a second antegrade motion [0.41 mm (SD 0.33)] in diastole, see Figure 2. Although the pattern is individual, the most common looks like the above described and presented in Figure 2, i.e. a larger retraction (retrograde movement) than the first motion forward (antegrade movement). The mechanisms responsible for this bidirectional movement is however undetermined and the complexity suggests that several interacting factors are involved. The arteries are tethered⁴ to the surrounding tissue by the arterial side branches and the perivascular connective tissues. The arteries are also under a natural condition of longitudinal tension.

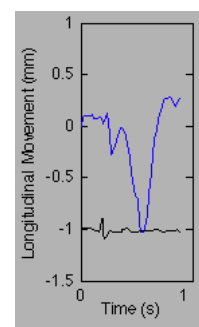


Figure 2: *Longitudinal movement in the carotid arterial wall over one cardiac cycle.*

The pressure wave from the heart formed in every heart beat could have an impact on the antegrade longitudinal movement. Moreover, it can not be ruled out that a local active force is affecting the motion of the vessels. Another hypothesis is that a shear force originated from the pulsatile blood flow acting parallel to the vessel wall could be an important factor for the motion in the antegrade direction. That alone can itself although not explain the retrograde motion. A theory is that a reflection of the pressure wave could have an impact. The carotid artery is divided into two separate paths just below the cheek. In this bifurcation the pulse wave naturally will suffer some reflection that could implicate a shear force parallel to the vessel wall in the retrograde direction. The retrograde motion could also be a recoil of the antegrade motion, since the vessels are tethered.

Another theory of the retrograde longitudinal movement is the fact that the heart has a similar movement pattern during the cardiac cycle. After the Electro-Cardio Gram (ECG) excitation and the beginning of contraction of the ventricles a distinct vertical movement is begun. The base of the heart moves toward the ventricular apex in systole⁵ and the heart is vertically dislocated approximately 12-17 mm downwards in systole followed by a motion upwards approximately 2/3 of the downward travelled length where it stays during diastole, and finally completed with an upward motion the remaining length to its original position just before the beginning of the next cardiac cycle.

The idea here is that this motion of the heart has the potential of straining the vessels a sufficient length for the longitudinal movement in the vessel wall to occur in the carotid artery. Thusly; this study will aim to investigate whether a correlation, between the vertical dislocation of the heart and the longitudinal movement in the carotid arterial wall during the cardiac cycle, exists.

For this manner, fourteen voluntarily enrolled subjects' heart movement and carotid longitudinal movement was examined and measured with ultrasound and evaluated. The data were analyzed in Matlab[®] 2010b (The MathWorks Inc., Natick, MA) and in HDILab[®] (Philips Medical Systems, ATL Ultrasound, Bothell, WA).

First an introduction to the wonders of ultrasound, followed by the methods of gathering the data, the procedure of analysis and finally the results of said analysis and a discussion.

1.1 Ultrasound

Ultrasound is a widespread technique, utilized in a number of fields. In the maritime industry it is commonly used as a depth measuring device and in the military navy, submarines rely entirely on what their sonar has to tell about the surroundings. The largest deployment of the ultrasound technique is, however, in the medical industry. Medical treatment applications like kidney stone lithotripsy, where a high energy ultrasound pulse is used to break urological stones, exists and is widely used but it is in medical imaging for diagnosis purposes the utilization has reached its largest spread, and it is this area the following mainly will focus on.

Diagnostic ultrasound imaging is a pulse-echo technique. This means that a small burst of ultrasound is sent, through the skin, into the patients body where it is reflected on the interfaces of the organs and travels back to its origin. The transducer, from which the pulse was sent, now acts as a receiver, recording the incoming echoes. With the knowledge of the propagation velocity of the sound pulse and the elapsed time between sent pulse and received echo, the distance between the transducer and the reflecting organ can be calculated. In this way a line of dots representing echoes at different depths is constructed, and by combining several lines adjacent to each other a two dimensional (2D) image is gathered representing a cross-section of the body.

1.1.1 Wave propagation

The sound wave is a longitudinally propagating wave. This can be described as an oscillation alternately pushing (compressing) and pulling (decompressing) the adjacent particles. The particles are set in motion and will begin oscillating like the source and start distributing the pushing and pulling to its neighbours allowing the sound wave to travel. Thusly, the particles move back and forth in the same direction as the wave propagate, creating bands of compressions and rarefactions. Although the wave travels, there are no net movement of the particles, they only oscillate around their balancing point generating these regions of high and low pressure.

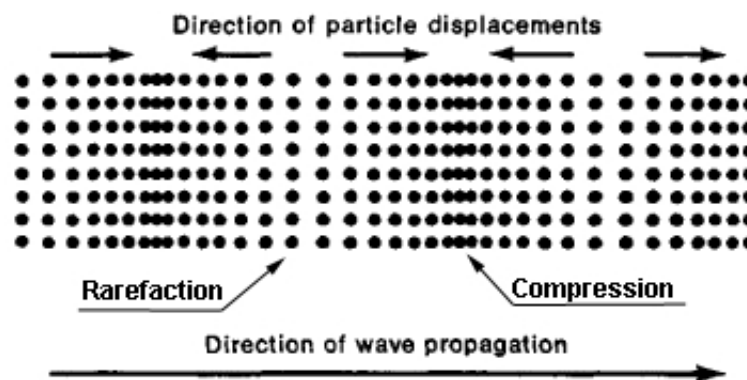


Figure 3: A longitudinal wave

Since the sound wave propagation is dependent of the particles in its way, the speed of sound, c , will vary depending on the properties of this medium. The two most significant properties of the medium, that affect the speed of sound, is the density, ρ , and the stiffness k ,

related by the formula $c = \sqrt{k/\rho}$. Consequently the speed of sound in gases, which have a very low stiffness, is relatively low, e.g. air $c_{air} = 333 \text{ ms}^{-1}$, whereas it for solids, with a significantly larger stiffness, is higher, like steel⁶ $c_{steel} = 5790 \text{ ms}^{-1}$.

For human tissue which is both denser than gases and thinner than steel, naturally, the speed of sound lies in between. In Table⁷ 1 some values for the speed of sound in typical organs can be seen. It is evident that these values do not differ that much from one and other. In fact they are similar enough that, for medical imaging purposes, the average value of 1540 ms^{-1} is assumed in the calculation process.

Be that as it may, the speed of sound in bone, with high stiffness, and in air, with low stiffness, differ remarkably from this average value with implications discussed later.

Material	c [ms^{-1}]
Liver	1578
Kidney	1560
Fat	1430
Water	1480
Bone	3190-3406
Air	333

Table 1: The speed of sound in typical mediums within the human body

1.1.2 Reflection

As mentioned before (1.1), the ultrasound image is constructed of echoes reflected from the boundaries between different tissues. If the body would be completely homogenous it also would be transparent to ultrasound. The small differences in the speed of sound between the organs, displayed in Table 1, is actually of crucial importance to their visibility in the ultrasound image. When an incident ultrasound pulse, traveling through a medium with one speed, encounters an interface of a different medium with a different speed of sound, a part of the energy in the pulse will be reflected whilst the remainder will be transmitted. This gives rise to the term acoustic impedance. The acoustic impedance is a measure of the particles ability to move, in terms of velocity, under a certain amount of pressure. As discussed before (1.1.1) the density, ρ , and the stiffness, k , are two parameters that affects the speed of sound in a given medium, and in this case the acoustic impedance, z , is governed by the equation, $z = \sqrt{\rho k}$, which, with the former equation for speed of sound, reduces to, $z = \rho c$. So for two neighboring organs, a difference in their individual acoustic impedance is required to make them distinguishable from one another. When a sound wave hits an interface, the amplitude of the incident pulse is therefore divided between a reflected and a transmitted pulse with a ratio dependent of the acoustic impedances of the two different mediums. This ratio, often called the amplitude reflection coefficient, R_A , is defined by:

$$R_A = \frac{z_2 - z_1}{z_2 + z_1}$$

Interface	R_A
Liver-kidney	0.006
Kidney-spleen	0.003
Blood-kidney	0.009
Liver-fat	0.11
Liver-bone	0.59
Liver-air	0.9995

Table 2: Amplitude reflection coefficients of interfaces in the human body

Where z_1 is the acoustic impedance of medium 1, and z_2 is the acoustic impedance of the second medium.

In Table⁸ 2 values of R_A for common interfaces in the human body is displayed. From Table 2 it is evident that in soft tissue to soft tissue interfaces, like liver-kidney, the reflection coefficient is fairly small, below 0.01 in these examples. This means that most of the energy of the pulse is transmitted further through the tissue with the ability to give rise to echoes from interfaces at increasing depths. In the case of Liver-air interface the reflection coefficient is 0.9995, this means that 99.95 % of the incident pulse is reflected, making

it virtually impossible to detect anything behind any air filled cavity. It is for this reason it is important to use a particular ultrasound gel on the transducer head during examination. The gel is suited to resemble the acoustic impedance of the human skin to ensure ultrasound penetration into the body.

1.1.3 Attenuation

When the ultrasound pulse travels through the tissue setting the particles in its way in motion, as discussed above (1.1.1), it transfers some of its energy in every such encounter, this is known as absorption. Some of the energy is also scattered by small irregularities in the tissue, i.e. sent in arbitrary directions. This makes the pulse's energy to gradually fade out and eventually be fully attenuated by the medium. Consequently there is a maximum depth that can be visualized, dependent of the energy of the pulse and the attenuation in the tissue. The rate at which energy is absorbed is related to the frequency of the pulse. The pressure wave in the pulse transfers energy that makes the particles move backwards and forwards and at low frequencies the particles move harmonically with the alternations in pressure, neatly transferring the energy back to the pulse. However, when the frequency increases the particles, due to their inertia, cannot keep up in the rapid fluctuations of the pressure wave, converting the transferred energy to heat in the tissue.

For diagnostic imaging purposes, the most commonly used frequencies range between 2-15 MHz. At large depths, when the attenuation is large, frequencies from the lower part of the interval must be used to ensure that the returning echos will be of sufficient energy to be able to visualize, whilst superficial targets, with benefits discussed later, can be detected with higher frequencies.

1.1.4 Transducer

As mentioned before (1.1) the ultrasound image is a composition of several lines of echoes that together forms the 2D cross section of the body. Every such line is produced by one ultrasound pulse that origins from a piezoelectric element. The piezoelectric element is a ceramic material which expands or contracts when it is exposed to a positive or a negative electric voltage, giving rise to the oscillations needed to produce the ultrasound pulse. The expansion and contraction is linearly proportional to the applied voltage. Contrariwise, the material generates an electrical voltage when compressed or stretched by an external force, translating the returning echoes from an acoustic wave into an electric voltage.

A common transducer called the linear array, consists of 128 piezoelectric elements in a row. To gather a 2D image the first element in the row is excited generating a ultrasound pulse that travels into the body. The element is then quickly altered to listening to the returning echoes for a time proportional to the depth of the body the image is supposed to reproduce. Subsequently, the same procedure is applied to the second element, and so forth until 128 lines has been collected. One image is consequently not produced instantly and the frame rate, i.e. number of images per second, is dependent of how deep we want to look, as stated above. To optimize the frame rate is obvious to not produce images at a depth exceeding the required. Another way of increasing the frame rate could be to only use every other element, which will double the frame rate but lead to a severely deteriorated image. The best way optimize the frame rate is to focus on a region of particular interest and only use the elements needed to visualize this area.

Another common transducer is called a phased array transducer. This transducer consists also of about 128 elements in row but for this model the elements are much more close together. The width of a phased array transducer is approximately one third of the width of a linear array transducer. Rather than sending the ultrasound pulses straight out perpendicular to the transducer head like the linear array does, the phased array sends the pulses in a fan shaped area. This makes the phased array transducer ideal for investigating objects with limited access, e.g. the heart. The ultrasound beam travels from the narrow head into a wide area of the body making it possible to get past the small passage between the ribs and yet cover a wide area below.

1.1.5 Resolution

The small burst of ultrasound, mentioned above, that is sent into the body is, naturally, not infinitely small but consists rather of a few oscillations around the nominal transmit frequency. The fact that it is expanded in time has consequences for the depth resolution. Two echoes separated a distance smaller than half the pulse's length can not be individually distinguished, and for this reason we want to minimize the pulse's length. However, as discussed before in 1.1.3, a low frequency is needed to be able to visualize deep targets. One always have to compromise between good resolution and good depth visualization.

The image consists of a number of lines as described in 1.1.4 and every line have some lateral expansion that increases the deeper the pulse travels due to diffraction. When a point target in the body is to be imaged several adjacent lines might be overlapping the same target due to their beam width. Subsequently the same point target will produce echoes to a number of lines, and since the system is not aware of the beam width every echo will be picturized as coming from the center of each line resulting in a stretched or smudged dot in the image. The lateral resolution is the smallest spatial distance two individual targets at the same depth can be separated from each other. Generally two targets can be just resolved in the image when separated by half the beam width.

1.1.6 Modes

There are two major ways of measuring and displaying ultrasound data. One is the Brightness-mode, (B-mode), which essentially is the procedure described above. In this mode either a linear array or a phased array is used to collect the data. With the linear array a rectangular area defined by the width of the array and the chosen depth, see 1.1.3, is scanned. The gathered data is also presented as a rectangle and represents a 2D cross section of the body. If a phased array is used the data is displayed as a cone proportional to the scanned area, see 1.1.4. The name Brightness-mode refers to that the brightness of a displayed dot in the image is proportional to the amplitude of the received echo.

Another mode is called the Motion-mode (M-mode). This is used to investigate motions over time within the body, e.g. heart movement. In this set up only one line in the transducer is used to collect data to the preferred depth which then is presented as a line on the display. After that the line is interrogated again and the line of data is presented next to the previous line on the display. This means that on the display we have time vs. depth rather than width vs. depth, such as the B-Mode configuration, on the axis of the image. That makes it possible to follow a single echo's motion over time if it moves in direction to or from the transducer.

1.2 Echo tracking

When the longitudinal movement in the common carotid arteries was discovered by Associate Professor Åsa Rydén Ahlgren, M.D., Clinical Physiology specialist, department of Clinical Physiology, Malmö University Hospital, Sweden, in 2002 it also became evident that the movement was impossible to measure with the existing instruments. The M-Mode (1.1.6) was of no use here since the motion essentially is perpendicular to the transducer, making it unaccessible for detection. Modern ultrasound machines is also equipped with the ability to detect doppler shift in the frequency from moving targets, but neither this could measure the movement with sufficient precision. Åsa Rydén Ahlgren approached Electrical Measurements, Faculty of Engineering, LTH at Lund University, Lund, Sweden, and came in contact with, among others, Prof. Kjell Lindström and Magnus Cinthio, a PhD student at the time, at the department working with research and development of new vessel characterization methods. A collaboration between the departments was initiated and Magnus Cinthio developed a method of motion measurement for arterial walls.

The method is an echo tracking technique that is using a two dimensional block matching algorithm to estimate motion of a preselected echo during a full cine loop. Block matching is commonly used technique to find matching blocks in a sequence of images. In this case it is used to detect pattern similarities of a small kernel in a region of interest (ROI) in subsequent frames of B-Mode ultrasound data. A distinct echo from irregularities in the arterial wall is selected in the first frame of the ultrasound data. The echo is enclosed with a region of interest (ROI) of selectable size, approximately 0.7·0.7 mm. Automatically, a kernel, with the size of one seventh of the size of the ROI, is set in the middle of the ROI. Thereafter is a search region, of the exact same size and location as the ROI, obtained in the following frame, which is then 2D cross-correlated with the ROI in the first frame. The cross-correlation delivers the location in the sequent frame that best fits the pattern of the echo selected by the kernel in the first frame. The ROI is then translated to the new position, given by the cross-correlation, in the second frame whereafter the algorithm starts over and cross-correlates with a search region in the third frame and so forth. To improve motion resolution the ROI in the first frame and the search region in the second frame is interpolated by a factor of 10. By this procedure a single echo can be tracked over a full cine loop of ultrasound frames containing vessel movement data of many cardiac cycles.

2 Methods

The aim of this study was to investigate the supposed correlation between the heart's vertical dislocation and the longitudinal movement in the carotid artery. It was therefore important to examine the two motions simultaneously at the same heart beats. Accordingly two separate ultrasound machines were required. One of which; a HDI[®]5000, Philips Medical Systems, ATL Ultrasound, Bothell, WA, equipped with a 35 mm wide linear array transducer, 5-12 MHz, to measure the longitudinal wall movement in the carotid artery. The machine was preset to acquire B-Mode data with one transmit focus zoomed in to a 20 mm frame width which gave a frame rate of 55 Hz. The lateral and axial resolution were both 20 pixels/mm and the persistence was turned off. The other machine was of the same model but equipped with a phased array transducer, 2-4 MHz, and preset to acquire M-Mode data of the heart movement at a frame rate of 100 Hz. To have some sort of base to emanate from in the post processing the ECG was also measured, with a frame rate of 100 Hz.

The examination was conducted on 14 healthy, normotensive, nonsmoking, females and males, with no history of cardiovascular disease, in the age between 20 and 35. All subjects gave informed consent to the Helsinki Declaration, and the study was approved by the Ethics Committee of Lund University.

Since breathing has a known impact⁹ on the pattern of the longitudinal wall movement in the carotid artery, it was of importance that the subjects would hold their breath during the recordings of the movement. All measurements was performed in a quiet room with the subject in the supine position after at least 15 minutes of rest prior to the start of the examination. All subjects were examined by the same experienced ultrasound technicians.

The examination was carried out in the following manner for each subject of investigation:

1. The ECG electrodes were appropriately put in position on the chest.
2. The phased array transducer for the M-Mode data of the heart movement was put in position just below the ribs at the left side of the abdomen. The transducer was adjusted to acquire echoes from the septal side of the left ventricle close to the origin of the aorta ascendance.
3. The linear array transducer was put in position 2-3 cm proximal to the bifurcation on the right side of the neck and adjusted to acquire fine echoes from the carotid artery.
4. When both transducers was properly tuned to supply echoes of sufficient quality the subject was asked to give a sign of being ready to hold their breath.
5. When the sign came the recording on both machines were started. To ensure that this happened simultaneously the recording was initiated with a simple count down of the kind: "3-2-1-Go!".
6. A recording was made for five seconds and was stopped simultaneously with a similar count down.
7. Steps 4-6 were repeated at least three times to make sure that data of sufficient quality was acquired in the occasion of a unknown failure.

8. The position of the linear array was changed to instead examine the left side carotid artery and adjusted accordingly.
9. Steps 4-7 were repeated.

All recordings was automatically saved with a filename containing a time stamp to make it possible to associate recordings of the heart movement with the concurrent recording of the carotid artery.

2.1 Analysis

To ensure that the two investigated movements was measured from the same base, the ECG-data was of vital importance. All measurements that pertain to the time emanates from the ECG data and both the longitudinal carotid artery wall movement and the movement of the left ventricle was measured from the peak value in the QRS-complex during each cardiac cycle.

2.1.1 Heart movement

The analysis of the heart movement was made in the program HDILab[®] (Philips Medical Systems, ATL Ultrasound, Bothell, WA) which is a post processing application designed for off-line cine loop analysis. The program displays the M-mode data aligned with the ECG data below, see Figure 4. The curve of echoes represent the position of the heart , i.e the distance

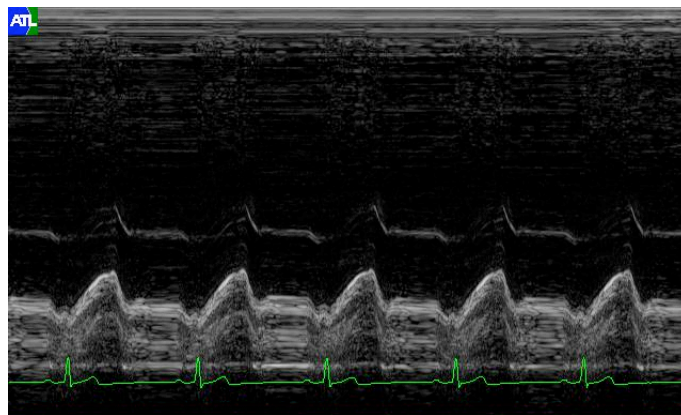


Figure 4: *M-Mode data of vertical heart movement. ECG data represented by green line.*

from the transducer, during several cardiac cycles. The transducer was held just below the ribs pointing upwards and since the measurement was performed from below, the peaks in the M-mode data represents a motion downward, to the stomach, of the heart and the troughs represent a motion upwards. In collaboration with Åsa Rydén Ahlgren the positions of the heart's movement of interest was determined.

These are:

1. The initiation of the retraction of the heart.
2. The point where the heart has reached its most retracted position.
3. The point where the heart has regressed to some state of equilibrium.
4. The point the equilibrium stops and the heart returns to its starting point for the next cardiac cycle.

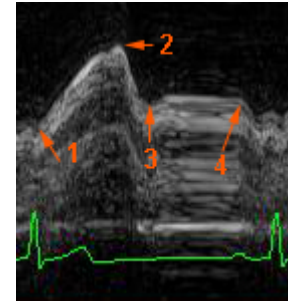


Figure 5: Vertical positions of the heart during one cardiac cycle. Position of interest marked by numbers and described to the left.

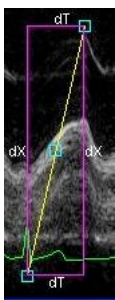


Figure 6: Measurement from peak ECG to point 2, list in Figure 5.

These points represent various vertical locations of the heart during the cardiac cycle. With the built in measurement tool “Distance M-Mode”, which also allows time measurement, the elapsed time from the top peak of the QRS-complex in the ECG-data to each of these positions of the heart was measured, for each cardiac cycle, see Figure 6. In some cases the M-mode data was too blurred or for other reasons not of sufficient quality to be able to measure in one or more of the above stated points. In those cases the entire cardiac cycle containing that or those points were excluded from further investigation. In addition the dislocation of the heart for each cardiac cycle was measured, again using the built in tool “Distance M-Mode”. Two distances were measured, the first is the maximum retraction from the initial position i.e. between point 1 and point 2 in the list in Figure 5, and the second is the distance from the point of maximum retraction, point 2, to the point where the heart stays steady for a while, i.e. point 3 also in the list in Figure 5.

2.1.2 Carotid artery wall movement

The movement of the carotid artery wall was measured using the above described block matching technique (1.2) implemented in a Graphic User Interface (GUI) in MATLAB R2010b. As explained, the algorithm tracks a user selected echo in a cine loop by cross-correlating subsequent frames. This means that the algorithm requires a distinct separable echo in the carotid intima-media complex during the entire interval of measuring to be able to fully track the movement.

The B-Mode ultrasound data received from the recordings were first exported to Matlab format using the, earlier mentioned, post processing application HDILab and then loaded in the GUI see Figure 7.

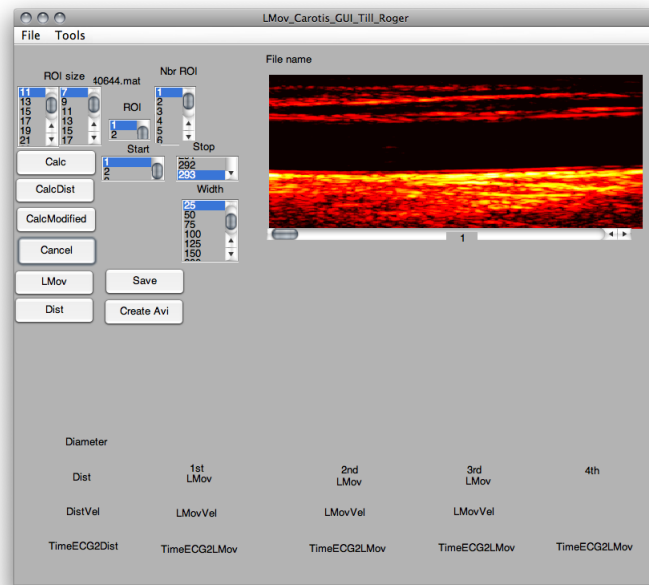
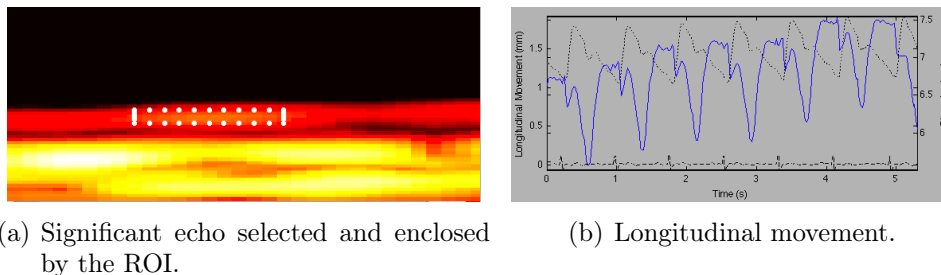


Figure 7: *Graphic user interface. The first ultrasound image of the cine loop of the carotid artery is visible in the upper right corner.*



(a) Significant echo selected and enclosed by the ROI.

(b) Longitudinal movement.

Figure 8: *Selected echo (a), and the longitudinal movement after tracking (b)*

After loading the file in the GUI the first frame of the cine loop became visible in the upper right corner. In the frame, a distinct echo, in the intima-media complex in the near wall of the vessel, was chosen by clicking with the mouse cursor. The frame was zoomable which made location and clicking of a significant echo easier. In the upper left corner of the GUI, see Figure 7, handles for resizing the ROI is visible. Each ROI was optimized in size to just enclose the chosen echo, see Figure 8(a). After pushing “CalcModified” and the video started, it was important to ocularly inspect the ROIs movement to make sure that it was locked to the echo of significance and followed through the entire interval. This to rule out the possibility for the ROI to lose its track of the chosen echo and instead leap and lock on an adjacent echo and thus presenting errors in coming calculations. After a complete tracking throughout the cine loop the longitudinal movement was automatically presented in a graph in the GUI (solid blue in Figure 8(b)) aligned with the ECG data (dashed curve at the bottom). Although not of importance for this study, the diameter change was also presented (dashed curve). By clicking on the first through in the graph where the initial antegrade motion starts the points on the curve presented in Figure 9 were automatically found and their individual time of occurrence from the preceding peak of the ECG were automatically calculated. The points are:

1. The peak of the QRS-complex in the ECG data.
2. Initiation of antegrade movement.
3. Initiation of retrograde movement.
4. The point where the carotid arterial wall has reached its most retracted position.
5. The point where the carotid arterial wall has regressed to its initial position.

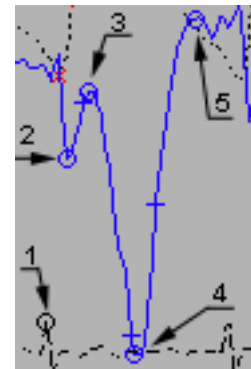


Figure 9: *Points of interest in the LMov data*

In Figure 10 the GUI is presented after completed calculations of all the measurable cardiac cycles in the interval. In the lower part of the figure the mean values of the time of occurrence, with corresponding standard deviation, is presented for each point of interest.

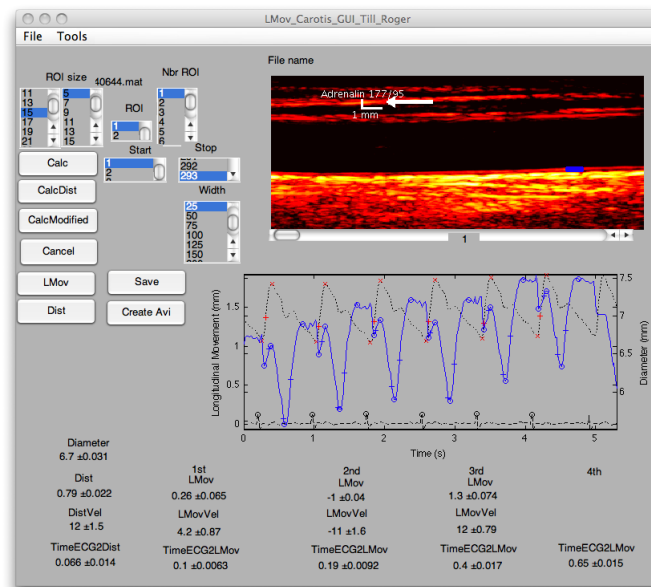


Figure 10: *The GUI when the longitudinal movement has been calculated for each cardiac cycle.*

2.1.3 Order of occurrence

It was desirable to measure the velocity of propagation of the retraction. An attempt to do this was made by measuring the longitudinal movement in two different points of the vessel wall. In this manner a difference in time of occurrence of the different points of interest described above was hoped to be found. If the antegrade motion in the carotid artery in a position close to the heart would precede the antegrade motion in a position further away, close to the bifurcation, from the heart, this would suggest that the motion is initiated in the heart region and travels out against the peripheral parts of the cardiovascular system. Similarly would a retraction of the vessel wall in a point close to the heart that precedes the same retrograde motion in a point further away, suggest that also this motion has its source in the region of the heart, and thereby underpin the theory about the heart movement being the mother of the carotid artery movement.

To effectively measure the longitudinal movement a distinct and stable echo was needed during the entire interval, as explained above. In this case, however, two distinct echoes from the same examination, advantageously placed as far apart as possible, were needed. Unfortunately, not all examinations of the subjects was of this virtue. Only four recordings was found to give the opportunity of measuring the longitudinal movement in two individual positions.

As explained before in 1.1.4 the image is composed of several lines that each takes some time to produce. This gave rise to the frame rate, or Frames Per Second (FPS), and leads to a postponing of the information in the image. Since the image is constructed from left to right, the information to the left of the image will be older than the information to the right when the image is presented on the screen. The postponing is naturally dependent of the number of lines used and the time each line takes to produce, i.e. the FPS, and to measure and compare movement in different parts of the image with precision this was needed to be compensated for. A correction term, based on the pixel position of tracked echo, was calculated:

$$correction = \frac{1}{FPS} \cdot \frac{pixPos}{numPix}$$

where FPS is the Frames Per Second value, $pixPos$ is the longitudinal pixel position of the echo and $numPix$ is the total number of pixels on the longitudinal axis. Two correction terms was calculated, one for the echo close to the heart and one for the echo close to the bifurcation, and then subtracted from their individual time vectors of the longitudinal movement.

3 Results

3.1 Movement

In total eight subject's data were possible to fully analyze. Fully meaning that the heart movement, the left side carotid arterial wall movement as well as the right side carotid arterial wall movement was measurable for an acceptable number of contiguous cardiac cycles. For the other subjects one or more of the three examinations were corrupted or in some other way of insufficient quality to be purposeful to investigate. However, among the remaining six subjects, two subject's heart movement data was of too low quality to analyze, and thereby of no further interest of investigation. The other four subject's heart movement together with either the left or the right carotid arterial wall movement were measured.

As explained in 2.1 the time to four different stages of the heart movement, and the time to four different stages of the longitudinal movement in the carotid artery wall, were measured from the preceding peak in the ECG for each cardiac cycle. The moved distance from the initial position of the heart was also manually measured in two different stages. The heart movement (red line) was then associated with the concurrent carotid movement (blue line) and superimposed in the same plot, presented for one subject in Figure 11. In the figure has the heart movement been reduced by a factor 20 and is consequently in reality in the order of centimeters. This was done to fit both measurements in the same plot and give a better graphic presentation of the prevalent circumstances.

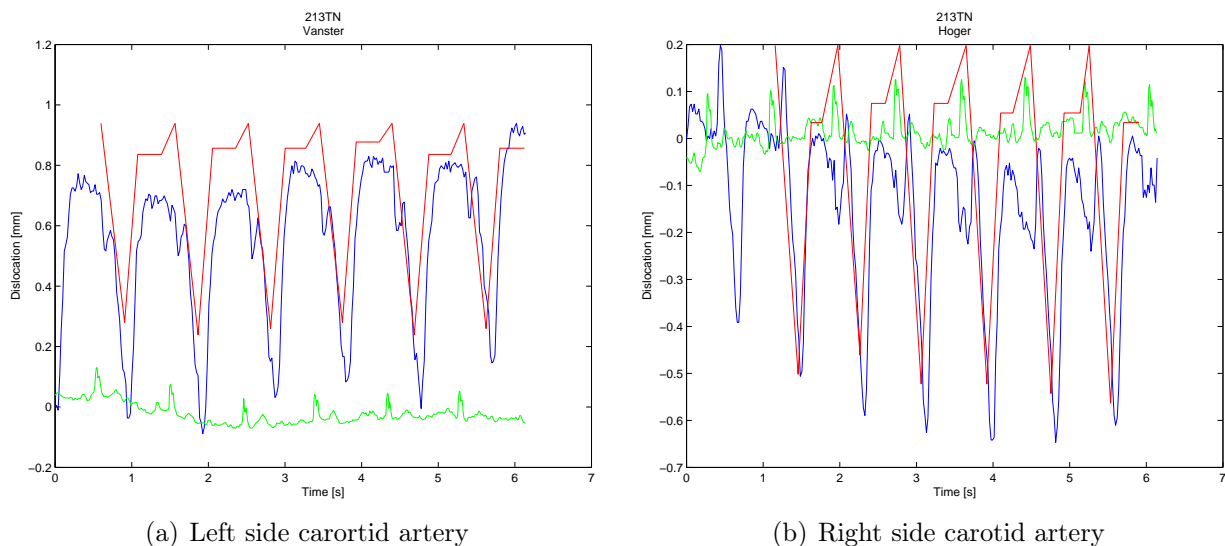


Figure 11: *The longitudinal arterial wall movement (blue line) of the left side (a), and of the right side (b), with the corresponding heart movement (red line) superimposed for each cardiac cycle. The ECG is also visible as a green line. The movement of the heart has been reduced by a factor 20 to better visualize the desired.*

Figure 11(a) represents the left side carotid artery wall motion with corresponding heart movement and Figure 11(b) represent the movement on the right side. For both sides it can be seen that both the start of the retraction and the start of the returning in the carotid arterial wall is preceded by the heart movement for each cardiac cycle. In Figure 12 a magnification of two areas covering two cardiac cycles in Figure 11(b) can be seen. In this magnification it is

quite unambiguous that the start of retraction of the heart precedes the start of retraction in the carotid artery, Figure 12(a). It is also clear that the point where the heart starts its regress likewise precedes the reversion in the carotid artery, Figure 12(b).

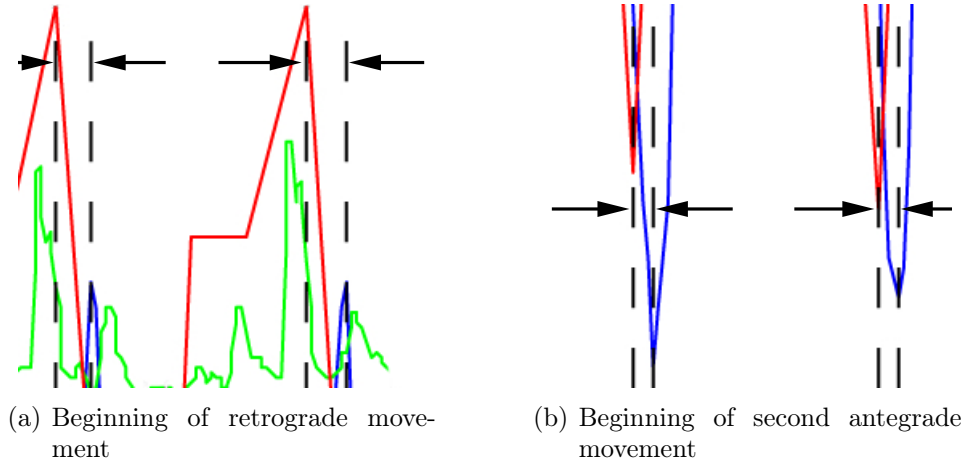


Figure 12: *It is clear that the retrograde movement in carotid artery (blue line) is preceded by the retraction of the heart (red line), subfigure (a). In (b) it is also clear that turning of the heart precedes the turning of the longitudinal movement. Both figures are magnifications of Figure 11(b)*

In Table 3 the difference in time, between the beginning of the movement in the carotid arterial wall and the beginning of the movement of the heart, for each analyzed heartbeat is visible. For almost every heartbeat for all subjects the retrograde movement in the carotid arterial wall starts at approximately 0.1 – 0.15 s after the heart has begun to dislocate downwards. Correspondingly it can be seen that the second antegrade movement of the carotid arterial wall starts after the heart has begun its movement upwards. It is for almost all subjects below 0.1 s after the heart and in most cases ≈ 0.05 s.

Side	Subject 1				Subject 2				Subject 3				Subject 4			
	Right		Left		Right		Left		Right		Left		Right		Left	
Movem.	Retrogr.	Antegr.	Retrogr.	Antegr.	Retrogr.	Antegr.	Retrogr.	Antegr.	Retrogr.	Antegr.	Retrogr.	Antegr.	Retrogr.	Antegr.	Retrogr.	Antegr.
Pulse 1	0.102804	0.01474	0.182112	-0.0063	0.119419	-0.01847	0.119622	0.042086	0.102401	0.043265	0.124167	0.075103	0.004298	0.017466	0.15112	0.011912
Pulse 2	0.123265	0.025201	0.161689	0.023801	0.123251	-0.00446	0.113048	-0.00449	0.117745	0.068609	0.120452	0.061316	-0.00349	-0.00047	0.154035	0.014827
Pulse 3	0.123584	0.045696	0.162289	0.054577	0.13703	0.009318	0.086624	0.019264	0.103118	0.063982	0.126709	0.077573	0.079476	0.02194	0.106875	0.027811
Pulse 4	0.103903	0.036015	0.153541	0.015653	0.140835	0.013123	0.101065	0.023529	0.128403	0.079195	0.122733	0.083669	0.061595	0.044411	0.10979	0.030726
Pulse 5			0.125041	0.027505					0.093965	0.084901	0.159032	0.089824	0.154479	0.036415	0.112704	0.02364
Pulse 6									0.11941	0.060202	0.165158	0.09595			0.125683	0.026619
Pulse 7									0.124493	0.055285						
Side	Subject 5				Subject 6				Subject 7				Subject 8			
	Right		Left		Right		Left		Right		Left		Right		Left	
Movem.	Retrogr.	Antegr.	Retrogr.	Antegr.	Retrogr.	Antegr.	Retrogr.	Antegr.	Retrogr.	Antegr.	Retrogr.	Antegr.	Retrogr.	Antegr.	Retrogr.	Antegr.
Pulse 1	0.13055	0.052635	0.105571	0.015795	0.133512	0.029319	0.082461	0.014546	0.121833	0.05447	0.109741	0.051826	0.113489	0.065574	0.106885	0.03897
Pulse 2	0.136454	0.058539	0.107283	0.017507	0.122788	0.028595	0.088971	0.029195	0.141151	0.055743	0.104793	0.056878	0.136708	0.032515	0.129408	0.033354
Pulse 3	0.22311	0.026361	0.100797	0.02916	0.142006	0.047813	0.10181	0.042034	0.142398	0.085035	0.103481	0.073705	0.093677	0.027623	0.121985	0.05407
Pulse 4	0.128348	0.048572	0.114254	0.032617	0.151223	0.05703			0.153619	0.086256	0.138475	0.034282	0.106896	0.058981	0.124507	0.076592
Pulse 5	0.114281	0.054505	0.12585	0.054213	0.150499	0.056306			0.158697	0.073289	0.120828	0.071052				
Side	Subject 9				Subject 10				Subject 11				Subject 12			
	Right		Left		Right		Left		Right		Left		Right		Left	
Movem.	Retrogr.	Antegr.	Retrogr.	Antegr.	Retrogr.	Antegr.	Retrogr.	Antegr.	Retrogr.	Antegr.	Retrogr.	Antegr.	Retrogr.	Antegr.	Retrogr.	Antegr.
Pulse 1	0.138113	0.005781					0.121799	-0.00053	0.135933	0.039879					0.14683	0.080776
Pulse 2	0.120139	0.024085					0.135209	0.012877	0.127908	0.041854					0.143373	0.085458
Pulse 3	0.142064	0.027871					0.138574	0.026242	0.148022	0.053829					0.128106	0.100191
Pulse 4							0.132028	0.009696	0.140023	0.063969					0.160952	0.094898
Pulse 5							0.135437	0.023105	0.151973	0.04778					0.147521	0.099606
Pulse 6							0.14703	0.024698								

Table 3: The difference in time, for every measurable cardiac cycle, between beginning of movement in carotid arterial wall and beginning of movement of the heart for two different stages, the retrograde movement and the second antegrade movement. For both right and left side carotid artery for the eight fully analyzed subjects, and for either left or right side for the remaining four subjects. All times in [s].

3.2 Order of occurrence

The attempt to measure and calculate the propagation velocity of the retrograde movement described in 2.1.3, failed to succeed. This was mainly due to a too low FPS that led to a poor time resolution. The poor time resolution introduced too big uncertainties in the calculations to make them useful. The movement itself, however, can be qualitatively examined for the four subjects that was possible to analyze. In Figure 13 we can see the longitudinal movement of the carotid arterial wall in two different points for one subject. The red line is the movement in a point close to the heart and the blue line is the movement in a point close to the bifurcation. Figure 13 shows that both the antegrade and the retrograde motion initiates close to the heart and travels out to peripheral parts. This is valid for every measurable subject.

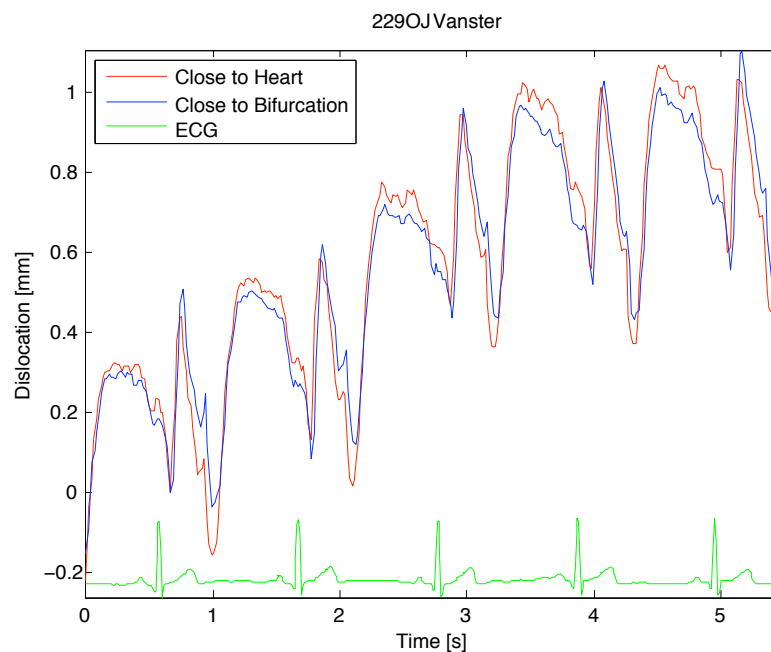


Figure 13: *The longitudinal movement measured in two different echoes. Its quite noticeable that the motion close to the bifurcation, in both the antegrade and the retrograde way, is preceded by the motion close to the heart, in every cardiac cycle*

Figure 13 clearly suggests that both the movement in the antegrade as well as in the retrograde direction is initiated from a mechanism that originates from the heart region.

3.3 Side to side comparison

In a comparison between the time of occurrence of the right and the left side carotid arterial wall movement of the point of release, i.e. the point where the wall has reached its most retracted position and is released to accomplish the last antegrade movement (Point 4 in 2.1.2), it gives a suggestion that the movement in the right side precedes the movement on the left side. In Figure 14 boxplots for the eight fully analyzed subjects', left and right side, are visible. The time from ECG to release for each cardiac cycle is represented by the boxes. The horizontal bar in the middle of each box is the median, the edges of the boxes are the 25th and 75th percentile and the whiskers extend to the most extreme values. Data points considered outliers are plotted individually.

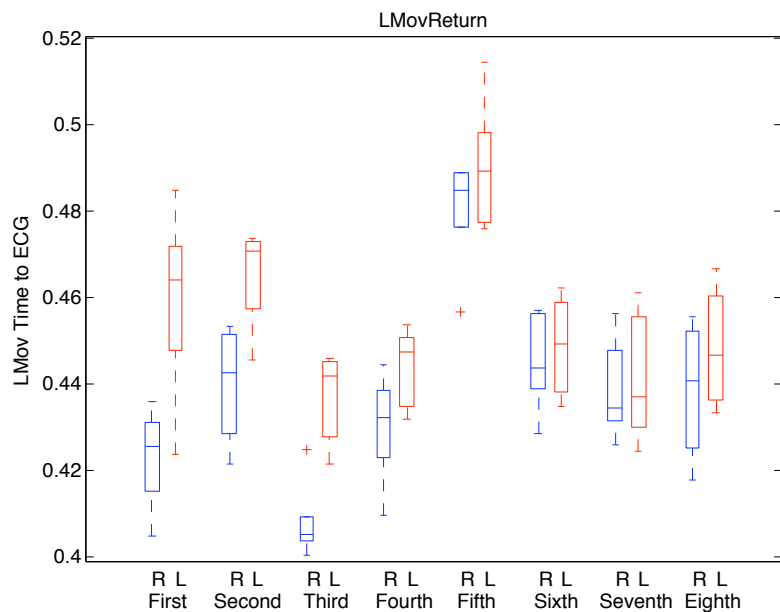


Figure 14: A boxplot for each subject's right and left side final antegrade carotid arterial wall movement. Time is measured from the ECG for each cardiac cycle. Blue boxes represent the right side movement whilst the red boxes represent the left side.

It is quite clear that the medians for every subject's right side carotid artery wall movement precedes the median of the left side movement, suggesting that the two data sets, left and right, comes from distributions with non equal medians.

A Wilcoxon signed rank test was also performed. The test performs a paired, two sided rank test of the null hypothesis that the two data sets comes from a continuous symmetric distribution with zero median. The test was carried out via the built in statistics tool box within Matlab 2010b. The Wilcoxon test delivered a rejection of the null hypothesis with the p-value:

$$p = 0.0078$$

which is well below the $p = 0.05$ that is required for the 5% significance level.

With this in mind it would be quite fair to say that the movement in the carotid artery on the left and right side, respectively, occurs with different delays from the ECG during each cardiac cycle.

4 Discussion

It seems that the heart's movement do play a crucial part in the movement of the carotids and there are mainly three different parts of evidence that point in this direction, these are:

1. The longitudinal movement is preceded by the heart's movement in every instance.
2. The movement of the carotid arterial wall in a point further away from the heart is preceded by the movement in a point closer to the heart. This is valid for the retrograde as well as the antegrade motion.
3. The second antegrade movement of the carotid arterial wall occurs on the right side before it occurs on the left side.

The analysis of all the subjects' retrograde longitudinal movement in the carotid arterial wall showed that it in all cases happens after the heart has started to move downwards. Also the second antegrade movement in the carotid arterial wall were for almost all subjects preceded by the movement upwards of the heart, with the exception for few individual cardiac cycles. The retrograde movement of the carotid arterial wall starts approximately 0.1 – 0.15 s (with an overall median of 0.1262 s) after the heart has begun to move downwards. Since the elasticity of the vessel walls will allow the vessels to stretch and expand a certain length, this would be expected. The vessels are also tethered to the surrounding tissues to hold them in place and this too will prevent the movement to happen instantaneously. The second antegrade movement in the carotid arterial wall happens after a very short period of time after the heart has left its most retracted position and is on its way upwards. The movement occurs with an overall median of 0.039 s after the heart has released its stretch. When the heart is retracted to its lowest position the vessels will be fully stretched. When the heart then starts to travel upwards relieving the tension of the vessels it would be noticeable almost instantaneously in a point far from the heart.

One could imagine the vessels as two rubber bands being weighed down by a vertically pending mass, the heart. When the mass is in its highest position the rubber bands is relaxed and under no tension at all. The mass then starts its pending downwards and the rubber bands gets more and more stretched. Since they were completely relaxed just before and because of their elasticity the motion would not be noticeable in a point of the rubber bands far away from the mass, before the mass has travelled a certain length. On the other hand, when the mass is in its lowest position, the rubber bands are fully stretched and under massive tension. When the mass starts to travel upwards the rubber bands would be relieved of that tension immediately making the heart's motion noticeable almost instantaneously in every part of the rubber bands.

The in this case utilized method, using the built in measuring tool "Distance M-Mode", in the post processing application for time and distance measurements for the heart movement, offers poor resolution in both the time-axis (<0.01 s) and the distance-axis (<0.4 mm). The data is exportable to Matlab but my efforts trying to implement a calculation algorithm failed to succeed. I think that this is a quite serious draw back since the precision in particularly the measurement of time is of paramount importance. To improve the certainty of measurements in the aspect of time as well as distance I highly recommend further investigation of the possibility to implement such algorithms that can deal with the heart movement data in a better platform than what the HDILab application offers.

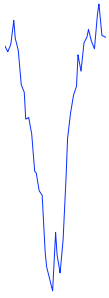


Figure 15: *The curve of the longitudinal movement is ragged in the most retracted position.*

The measurement point of beginning of retrograde motion in the carotid arterial wall seems to be of satisfactory precision. In the first calculations of when the carotid arterial wall starts to return from its most retracted position it became evident that the measurement point of the start of the second antegrade motion in some cases were wrong. The problem arises from a too low sample frequency which leads to an incorrect longitudinal movement curve, particularly in the regions of where the carotid wall has reached its most retracted position and is about to return. The calculation algorithm in the GUI of the longitudinal movement is preset to calculate this time from where the longitudinal movement is in its most retracted position and that point is not always necessarily the true position. In the event of a ragged appearance of the curve like in Figure 15, it is most likely that the

chosen point is wrong and thus also the time calculation. This was taken care of by tuning the algorithm to search for a point in the retracted position *and* where the subsequent curve was monotonically increasing. This adjustments dealt with most of the problematic cases, but still a few was not yet in the ultimate position, and thus, producing some minor flaws in the time measurements from this particular point.

Moreover is it clear that the motion in the carotids is caused by a mechanism in the region of the heart. In Figure 13 we doubtlessly can see that both the retrograde and the second antegrade motion happens in point closer to the heart than it does in a point further away. If it would be a reflection of the pulse wave or the blood flow in the bifurcation that caused the retrograde motion of the carotids, the motion would surely be noticeable next to the bifurcation before it would further away, close to the heart. This is not the case. The motion is initiated from below, and this definitively suggests that the heart is tearing the vessels backwards. When the heart later releases its tension of the vessels, and starts to move upwards, the vessels also begin to move upwards. Again the motion is begun in a point of the vessels that is close to the heart.

In 3.3 we also can see that, in the comparison between the time of antegrade movement in the carotids of the left and right side, the movement on the right side most likely happens before the movement on the left side. Since the vessels on the right and the left side is of different lengths this is very comprehensible. The “wave” of motion, if one could say that, actually has to travel further on the left side than it must on the right side, and thereby the motion is visible on the right side carotid wall before on the left side. Once again this suggests that the motion is governed by the heart.

Maybe one would argue that also the beginning of the retrograde motion should be visible on the right side before the left side. This is however not the case in this analysis, the motion seems to happen on random. But this is not contradictory to the thesis. The beginning of the retrograde motion is a complicated phenomena where several forces are involved. The vessels are first moved in the antegrade direction by the shear force of blood flow or whatever force one believes, then there is the, supposedly, force of the heart in the retrograde direction, discouraging the antegrade force. In a certain moment the retrograde force conquers the antegrade force and the vessel wall starts to move backwards. This is however such a complex battle of forces making it impossible to predict.

All in all, three independent factors that all points in the same direction. Although they

individually may seem to be somewhat unsound proof, they together manifests' the thesis to a point where at least I am assured.

References

- ¹J. Blacher, A. P. Guerin, B. Pannier, S. J. Marchais, M. E. Safar, and G. M. London, "Impact of aortic stiffness on survival in endstage renal disease," *Circulation*, vol.99, pp. 2434-2439, 1999.
- ²W. W. Nichols and M. F. O'Rourke, *McDonald's Blood Flow In Arteries*, 4th ed. London: Edward Arnold, 1998.
- ³M. Cinthio, et al, "Longitudinal movements and resulting shear strain of the arterial wall," *Am J Physiol Heart Circ Physiol*, 291: H394-H402, 2006.
- ⁴W. W. Nichols and M. F. O'Rourke, *McDonald's Blood Flow In Arteries*, 4th ed. London: Edward Arnold, 1998.
- ⁵J. S. Simonson and N. B. Schiller. "Descent of the base of the left ventricle: an echocardiographic index of left ventricular function." *Am J Soc Echocardiogr*, 2:25-35, 1989
- ⁶<http://hyperphysics.phy-astr.gsu.edu/hbase/sound/souspe2.html>
- ⁷P. Hoskins, K. Martin and A. Thrush "Diagnostic Ultrasound physics and equipment," 2nd ed. p. 7, Cambridge University Press, 2010.
- ⁸P. Hoskins, K. Martin and A. Thrush "Diagnostic Ultrasound physics and equipment," 2nd ed. p. 9, Cambridge University Press, 2010.
- ⁹M. Cinthio, et al, "Evaluation of an Ultrasonic Echo-Tracking Method for Measurements of Arterial Wall Movements in Two Dimensions," *IEEE Transactions on Ultrasonics, Ferroelectrics, and Frequency Control*, vol. 52, No. 8, pp. 1300-1311, 2005.